Distorted-wave electron-impact-ionization cross sections for highly ionized neonlike atoms

S. M. Younger
National Bureau of Standards, Washington, D.C. 20234
(Received 27 August 1980)

Electron-impact-ionization cross sections have been computed for several neonlike ions in a distorted-wave Born exchange approximation. For lower ionization stages the total cross section was found to be sensitive to the details of the distorted potential in which the partial waves were calculated. Ionization from the $2s^2$ core subshell increased in importance for higher charge states. Isoelectronic curves are presented which allow the interpolation of nonrelativistic electron-impact-ionization cross sections for any ion in the neon sequence in the incident electron energy range of one to three times threshold. A comparison to available experimental and semiempirical formulas is made.

I. INTRODUCTION

Electron-impact-ionization cross sections for positive ions play an important role in understanding the evolution and structure of high-temperature plasmas. In astrophysics, such data are integral components of stellar models, as well as theories of interstellar media. Terrestrial applications include the detailed modeling and diagnostic programs now a part of the thermonuclear fusion effort.

Until recently, very little information on electron-impact-ionization of positive ions was available beyond the first one or two ionization stages. Although several semiclassical and semiempirical formulas have been proposed, they are completely untested in the region of high charge states and near threshold electron-impact energies.[1,2] It is of some importance, therefore, to investigate the application of *ab initio* methods to the ionization process with the goal of uncovering some systematic scaling rules which will allow extrapolation and interpolation of existing data, as well as a quantitative evaluation of the accuracy of the simple formulas.

Theoretical studies of the isoelectronic scaling of the electron-impact-ionization cross section have so far been made only for light sequences such as H (Refs. 3 and 4), He (Ref. 5), Li (Refs. 4 and 6), and B.[7] The present work investigates the Z dependence of the ionization cross section of neonlike ions, using the same distorted-wave Born exchange approximation previously applied to the H (Ref. 4), He (Ref. 5), and Li (Ref. 4) sequences.

The neon isoelectronic sequence is particularly well suited for such a study for several reasons. First, the closed-shell target is a many electron system which is represented fairly accurately by independent particle Hartree-Fock wave functions. It is not expected that target configuration-interaction effects will substantially affect the present results. Second, the role of electron-impact excitiation to autoionizing states which later emit an electron should be small compared to other atomic systems. The lowest autoionizing state in Na^+ accessible via dipole excitation is $2s2p^6 3p$, involving a transition between a deeply buried core orbital and a rydberg-like excited state. In more highly ionized atoms this state is bound and the autoionizing process can occur only for higher nl states which have small excitation cross sections. Inner-shell ionization is also limited to high incident energies for low ionization stages. See Fig. 1 for a comparison of the inner-shell excitation to the first ionization threshold. The neon sequence thus provides an opportunity to study a case of direct ionization from a many electron ion of relatively simple internal structure. The third reason for choosing Ne-like ions is that existing experimental cross section data on Ne *I* (Ref. 8), Na *II* (Ref. 9 and 10),

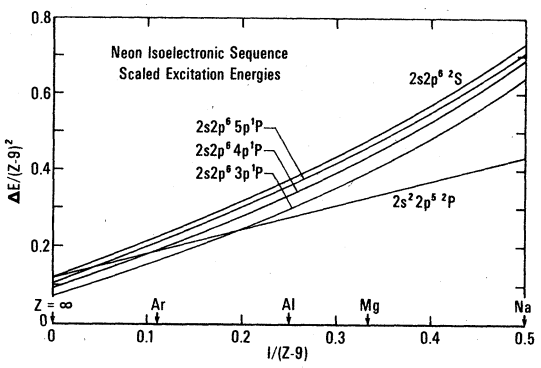

FIG. 1. Excitation energies (in rydbergs) scaled by the square of the effective nuclear charge $Z_e = Z - 9$. As Z_e increases, the threshold for $2s$ ionization decreases, with the $2s$ and $2p$ levels becoming degenerate at $Z_e = \infty$. Note that the $2s2p^6 3p$ state is bound for $Z_e > 14$ and that higher-p states fall below the $2p^5\,^2P$ limit at higher nuclear charges.

and Mg *III* (Ref. 11) indicate a departure from the classical scaling of the cross section by the square of the ionization energy, behavior which is followed in almost every other sequence for which data are available.[4-7] A significant motivation for the present work is to identify and evaluate such departures from simple scaling laws.

Section II is a brief review of the formal and numerical methodology employed. Section III presents the results of the calculations. Section IV contains a discussion of the calculations and the scaling laws, and compares the present work to other theoretical and experimental data. Section V is a summary.

II. METHOD

The application of the distorted-wave Born-exchange approximation to electron-impact ionization has been described in detail elsewhere.[4] Briefly, one employs partial-wave expansions for the wave functions representing the incident, ejected, and scattered electrons, with the partial-wave radial orbitals computed in some physically realistic yet computationally tractable potential. In previous work[4,5] on light ions a static potential was employed, consisting of the direct (local) terms of the Hartree-Fock Hamiltonian for the ground state of the target ion

$$V_D = -\frac{Z}{r} + \sum_{i=1}^{N} J_i(r) , \tag{1}$$

where Z is the nuclear charge, N is the number of target electrons, and $J_i(r)$ is the electrostatic potential due to the ith bound orbital

$$J_i(r) = \frac{1}{r}\int_0^r P_i(\rho)P_i(\rho)d\rho + \int_r^\infty P_i(\rho)P_i(\rho)\frac{1}{\rho}d\rho \tag{2}$$

with $P_i(r)$ the radial part of the orbital.

Preliminary work on Ne-like ions using the above potentials indicated very large phase shifts for p partial waves; phase shifts which were sensitive to the details of the distorting potential. In order to more accurately represent the lower l partials, we added to V_D a semiclassical exchange potential suggested by Riley and Truhlar[12]

$$V_{\rm SCE} = \frac{(V_D - E)}{2} + \tfrac{1}{2}[(E - V_D)^2 + \alpha^2]^{1/2} , \tag{3}$$

where E is the partial-wave energy in rydbergs and

$$\alpha^2 = \frac{4}{r^2}\sum_{i=1}^{N} P_i^2(r) . \tag{4}$$

The accuracy of this simple formula was checked by running parallel calculations using the author's frozen-core Hartree-Fock program with the partial wave iterated over the exchange integrals involving bound-continuum function pairs. A comparison of phase shifts (in radians) is given in Table I and demonstrates remarkable agreement between the semiclassical exchange (SCE) potential and Hartree-Fock methods.

For the target orbitals we employed the Hartree-Fock ground-state wave functions of Clementi and Roetti.[13] The incident electron partial waves were computed in the potential of the $N=10$ electron ground state:

$$V_I = -\frac{Z}{r} + 2J_{1s} + 2J_{2s} + 6J_{2p} + V_{\rm SCE}^{N} . \tag{5}$$

In the direct scattering matrix element the ejected (lower-energy) partial waves were computed in the potential of the final ion:

$$V_F = -\frac{Z}{r} + 2J_{1s} + 2J_{2s} + 5J_{2p} + V_{\rm SCE}^{N-1} , \tag{6}$$

where $V_{\rm SCE}^{N-1}$ is obtained from $V_{\rm SCE}^{N}$ by the omission of one $2p$ electron. The final (higher-energy) partial waves in the direct scattering matrix element were computed in the potential of the initial target V_I. Such a choice is in the spirit of the two-time model of inelastic scattering where the scattered electron is assumed to transit the region occupied by the ion in a time short compared to the rearrangement time of the target. In the exchange scattering matrix element, the final-state potentials are reversed—the ejected electron is computed in V_I and the scattered electron in V_F. Such a nonphysical choice is tolerated in order to insure orthogonality of overlapping orbitals in the matrix element, and has been found to yield theoretical data in reasonable agreement (better than 25%) with available experimental total cross sections of light ions. Note that for ionization of an inner-shell $2s$ electron, the final-state potential V_F considers six $2p$ electrons and one $2s$, in both V_D and $V_{\rm SCE}$.

TABLE I. Comparison of s-, p-, and d-wave phase shifts δ in Na^+ associated with frozen-core Hartree-Fock (FCHF) semiclassical exchange (SCE) and static (no-exchange) potentials (in radians).

Energy (Ry)	l	$\delta^{\rm FCHF}$	$\delta^{\rm SCE}$	$\delta^{\rm Static}$
0.04896	0	0.06857	0.05292	0.2023
	1	2.091	2.092	1.799
	2	0.1726	0.1746	0.06100
0.2172	0	0.05460	0.03742	0.2122
	1	2.069	2.069	1.782
	2	0.1945	0.1932	0.07087
0.3855	0	0.04099	0.02450	0.2218
	1	2.048	2.047	1.766
	2	0.2149	0.2111	0.08052

Partial waves were calculated numerically over a 350 point block-linear radial grid. For incident electron energies u less than or equal to 1.5 threshold units ($u=1$ threshold unit = ionization energy of target), the maximum partial-wave angular momenta included for the incident, ejected, and scattered waves were 10, 6, and 10, respectively. For $1.5<u\leq 3$ the maximum values were 13, 6, and 13, which were sufficient to insure convergence of the partial cross section series at all energies considered here. Radial matrix elements were computed by a double application of Simpson's rule. Integration over the ejected electrons' energy distribution was accomplished by a three-point Gauss-Legendre formula. The $Z=\infty$ cross sections are essentially scaled hydrogenic data, computed in the same approximation described above except for the use of $Z=1$ Coulomb functions for all orbitals.

Following our previous convention,[4,5] we employ the "maximum interference" approximation of Peterkop[14] for the phase of the exchange matrix element which is designed to maximize the effect of scattering exchange, and hence minimize the total cross section within the limits of the Born-exchange approximation.

Table II lists the ionization energies for $2p$ and $2s$ subshells of the neonlike ions studied in the present work. Where available, experimental data were used.[15-18] For Ar IX no empirical $2s$ energy was avialable; as an approximation we employed the $2s$ eigenvalue of the Clementi and Roetti Hartree-Fock calculation.[18]

Cross sections for excitation of the $2s2p^6 3p\ ^1P$ autoionizing state were calculated in the distorted-wave exchange approximation, with initial- and final-state partial waves computed in the potential of the initial target ground state, including semiclassical exchange. Experimental excitation energies and Hartree-Fock initial and final target states[19] were employed.

III. RESULTS

Electron-impact-ionization cross sections for highly ionized Ne-like atoms computed in the distorted-wave Born exchange (DBE) approximation are given in Table III. Cross sections for ionization of a $2s$ core electron and a $2p$ outer-shell electron are listed separately. Note that the $2s$ ionization cross section is much smaller than the $2p$. To suppress the gross Z dependence of the cross section we tabulate the classically scaled quantity $uI_{2p}^2 Q$ where u is the incident electron's energy in units of the $2p$ ionization energy $u=E/I_{2p}$. The energy range $u=1.125-3$ encompasses the most important energy range encountered in most plasma devices.

TABLE II. Ionization energies (in eV) used in the present work.

Ion	I_{2p}	I_{2s}	I_{2s}/I_{2p}
Na^+	47.29 [a]	80.09 [b]	1.69
Mg III	80.15 [a]	118.8 [c]	1.48
Al IV	120.0 [a]	164.5 [d]	1.37
Ar IX	422.5 [a]	498.0 [e]	1.18

[a] Reference 15.
[b] Reference 16.
[c] Reference 17.
[d] Reference 18.
[e] Reference 13.

Figure 2 is a Fano plot of the DBE scaled ionization cross section uI^2Q for Na^+ compared to the crossed-beam experimental data of Hooper *et al.*[9] and Peart and Dolder,[10] as well as the universal semiempirical formula of Lotz[20] and the Coulomb-Born no-exchange results of Moores.[21] Two distorted-wave curves are shown, illustrating the effect of the semiclassical exchange partial-wave potential on the total cross section.

Figures 3–5 are Fano plots of the scaled cross

TABLE III. Scaled electron-impact-ionization cross sections uI^2Q for highly ionized neonlike atoms in units of πa_0^2 (Ry)^2.

	$uI^2Q(2p^6-2p^5kl)$				
u_{2p}	Na II	Mg III	Al IV	Ar IX	$Z=\infty$
1.125	0.414	0.942	1.45	2.34	2.72
1.25	0.947	1.99	2.88	4.36	4.94
1.50	2.31	4.28	5.68	7.76	8.39
1.80	4.31	7.07	8.78	11.1	11.5
2.25	7.50	11.0	12.9	15.1	15.0
3.00	12.6	16.6	18.5	20.2	19.0
	$uI^2Q(2s^22p^6-2s2p^6kl)$				
u_{2p}	Na II	Mg III	Al IV	Ar IX	$Z=\infty$
1.125					0.707
1.25				0.236	1.30
1.50		0.130	0.194	0.959	2.26
1.80	0.0372	0.303	0.654	1.68	3.14
2.25	0.258	0.806	1.32	2.56	4.13
3.00	0.767	1.94	2.26	3.73	5.31
	Total cross sections				
u_{2p}	Na II	Mg III	Al IV	Ar IX	$Z=\infty$
1.125	0.414	0.942	1.45	2.34	3.43
1.25	0.947	1.99	2.88	4.60	6.24
1.50	2.31	4.41	5.87	8.72	10.7
1.80	4.34	7.37	9.44	12.8	14.7
2.25	7.76	11.8	14.2	17.7	19.1
3.00	13.3	18.6	20.8	23.9	24.3

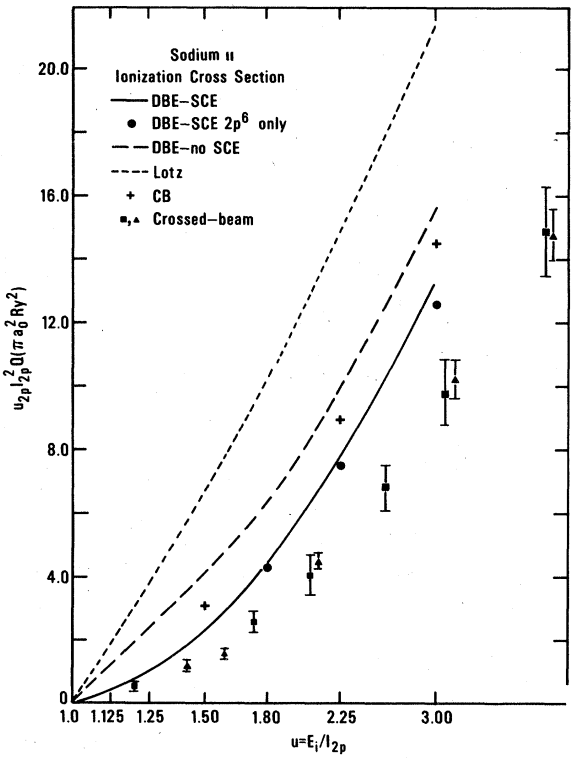

FIG. 2. Fano plot of the scaled electron-impact-ionization cross section uI^2Q for Na^+. ——— distorted-wave Born exchange including semiclassical exchange in the distorted potentials; — — — distorted-wave Born exchange without semiclassical exchange in the distorted potentials; ● same as solid line but omitting inner-shell ionization from $2s^2$; + Coulomb-Born no exchange, Ref. 21; ■ crossed-beam experiment, Ref. 9; ▲ crossed-beam experiment, Ref. 10; - - - Lotz semiempirical formula, Ref. 20.

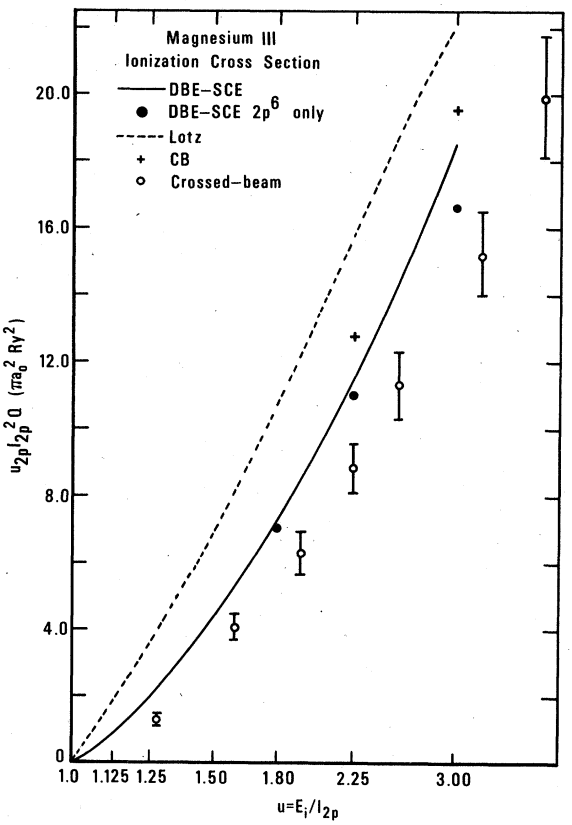

FIG. 3. Fano plot of the scaled electron-impact-ionization cross section uI^2Q for Mg III; ——— distorted-wave Born exchange with semiclassical exchange in the distorted potentials; ● same as solid line but omitting inner-shell ionization from $2s^2$; + Coulomb-Born no exchange, Ref. 21; ○ crossed-beam experiment, Ref. 11; - - - Lotz semiempirical formula, Ref. 20.

section for electron impact ionization of Mg III, Al IV, and Ar IX. Note that no comparison material, theoretical or experimental, is available for the highest two ions except for the semiempirical formula of Lotz.[20]

Figure 6 is an isoelectronic plot of the electron-impact-ionization cross section for Ne-like ions in the incident energy range $u = 1 - 3$. This type of plot is particularly useful in that it allows the ready interpolation of the nonrelativistic cross section for any ion in the neon sequence in the energy range considered. Each curve corresponds to a given energy in threshold units.

IV. DISCUSSION

A. Distortion effect

Comparison of the solid and dashed curves for the scaled electron-impact-ionization cross section of Na^+ in Fig. 2 demonstrates a significant dependence of the total cross section on the details of the distorted potential in which the partial waves are calculated. For Na^+ at $u = 1.125$ the addition of the semiclassical-classical exchange term to the static potential reduces the cross section by more than a factor of 3. The largest changes are found in the near-threshold region; at $u = 3$ the reduction is less than 15%. The effect for Mg III is much smaller; less than 10%, reflecting the increased rigidity of the wave function in the stronger Coulomb field. Table I demonstrates the effect of exchange on the phase shifts of $l = 0$, 1, and 2 ejected partial waves in Na^+.

In order to examine this sensitivity of the total cross section to the distorted potential more closely, a large number of parallel calculations were performed for Na^+, $u = 1.25$, using a wide variety of different potentials ranging from plane-wave Born to Coulomb Born to distorted wave. The result was that while the cross section was

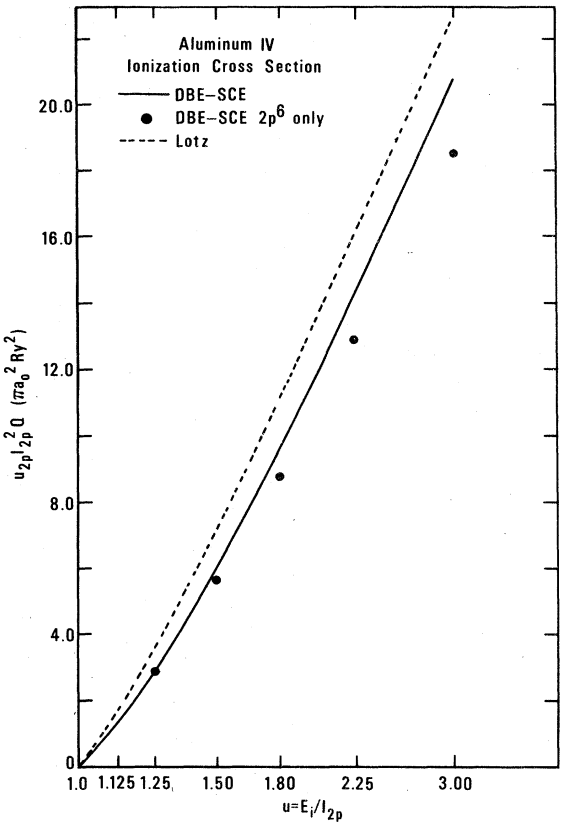

FIG. 4. Fano plot of the scaled electron-impact-ionization cross section uI^2Q for Al IV. ——— distorted-wave Born exchange with semiclassical exchange in the distorted potentials; • same as solid line but omitting inner-shell ionization from $2s^2$; - - - Lotz semiempirical formula, Ref. 20.

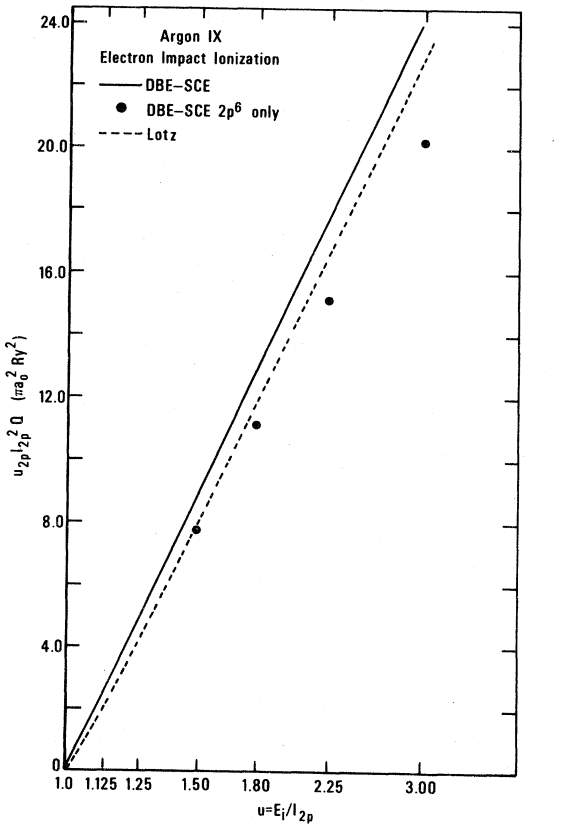

FIG. 5. Fano plot of the scaled electron-impact-ionization cross section uI^2Q for Ar IX. ——— distorted-wave Born exchange with semiclassical exchange in the distorted potentials; • same as solid line but omitting inner-shell ionization from $2s^2$; - - - Lotz semiempirical formula, Ref. 20.

very sensitive to the *ejected* partial wave, it was quite *insensitive* to the scattered and incident waves. Thus for the same ejected wave, the use of Coulomb waves or static distorted waves in the scattering states changed the cross section by less than 25% in the energy range 1-3 times threshold.

This sensitivity of the ionization cross section to the ejected partial wave mirrors the sensitivity of electron-impact-excitation cross sections to the accuracy of the initial and final target state.[22] In excitation, it has been found that for optically allowed excitations the most important factor influencing the accuracy of a distorted-wave cross section is the representation of the target states. In ionization, the ejected electron comprises the final "target" excited orbital and an analogous sensitivity is observed. Physically, the insensitivity of Q_{ion} to the scattering states reflects a weak coupling between the scattering electron and the target, and is supportive of the two-time

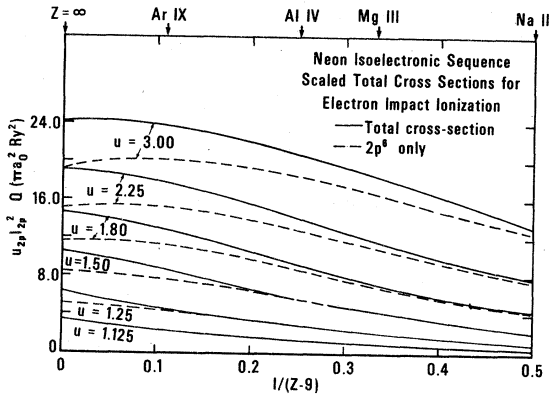

FIG. 6. Isoelectronic plot of the scaled electron-impact-ionization cross sections uI^2Q for neonlike ions computed in the distorted-wave Born-exchange approximation with semiclassical exchange in the distorted potentials. Each curve corresponds to a fixed incident electron energy measured in ionization threshold units $u=E_i/I$. ——— total ionization cross section; - - - cross section for ionization from the $2p^6$ subshell only.

model[23] of inelastic scattering where the scattering event is assumed to occur in a short time compared th the rearrangement time of the target. Such weak coupling supports the basic premise of the distorted-wave approach, that the target and scattered electron are weakly interacting even in the two continuum electron final state, and that in many applications where very near threshold ($u<1.1$) accuracy is not required, a simple independent particle representation can produce reasonable results. The problem of correlating many pairs of final-state partial waves is one of immense computational difficulty when approached within the conventional framework of many-body perturbation theory or continuum configuration interaction.

B. Isoelectronic behavior of the cross section

The significant departure of the total ionization cross section from classical scaling by the square of the ionization energy (Thomson scaling)[24] evident from Fig. 6 is in contrast to previous studies of the light isoelectronic sequence H (Ref. 4), He (Ref. 5), and Li.[4,6] At three times threshold the scaled ten-electron cross section varies by more than 50% between the first ion (Na^+) and the high-Z asymptotic limit. Note that there is an energy dependence to the scaling behavior, the lower isoelectronic curves being concave with respect to the abscissa while the higher-energy curves are convex.

Part of the increase in the scaled ionization cross section at high Z is due to the increased importance of inner-shell ionization for more highly ionized species. As the ionic charge increases, the threshold energy for $2s$ ionization decreases with respect to the primary $2p$ threshold energy, as is illustrated in Fig. 1. Since the $2s$ ionization cross section is zero at its own threshold and rises thereafter, the lower its ionization energy is with respect to the $2p$ threshold the larger the $2s$ contribution will be relative to the $2p$ at a given absolute incident energy. For Na^+ the $2s$ threshold is $1.69I_{2p}$ whereas for Ar IX, $I_{2s}=1.18I_{2p}$. For a given scaled incident electron energy of $3I_{2p}$, the equivalent energies in $2s$ threshold units are 1.78 for Na^+ and 2.54 for Ar IX. Since the scaled $2s$ ionization cross section curves for both ions follow the same general dependence on u_{2s}, one expects a larger contribution to the total ionization cross section for Ar IX than for Na^+. (The scaled cross section uI^2Q increases with u.) A plot of the ratio of the contribution of $2s$ and $2p$ ionization to the total cross section is given in Fig. 7.

Concurrent with the increasing importance of inner-shell ionization at higher charge states is

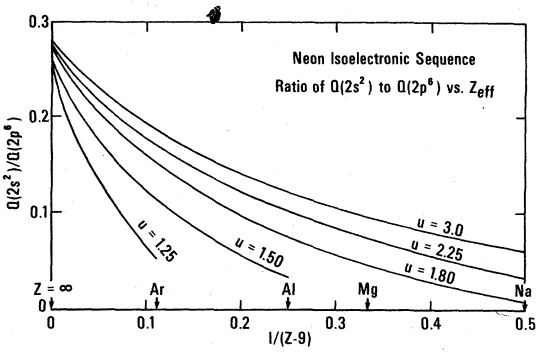

FIG. 7. Isoelectronic plot of the ratio of the electron-impact-ionization cross sections from inner-shell ($2s^2$) ionization to outer-shell ($2p^6$) ionization.

the possibility of discrete excitation to autoionizing states of the kind $2s2p^6np$ which later autoionize and thus indirectly contribute to the total ionization cross section; for Na^+, $\Delta E(2s^22p^6-2s2p^63p)=1.71I_{2p}$. Since the excitation cross section is small over the incident energy range considered here, the net influence of excitation+autoionization is less than 1% for this ion at three times the $2p$ ionization threshold. For Al IV the excitation energy is only $1.08I_{2p}$ so that, as in the case of $2s$ ionization, larger excitation cross sections occur at lower absolute incident energies. At Si V the $2s2p^63p$ level is bound, i.e., $E(2s2p^63p)<E(2s^22p^5)$, so that the first autoionizing state is $2s2p^64p$. Assuming smooth isoelectronic behavior of the $2s$-$3p$ and $2s$-$4p$ scaled excitation cross sections and scaling along the rydberg series np as $(n^*)^{-3}$ where n^* is the effective quantum number, one may expect excitation-autoionization processes to be *less* of a problem for Si V than for Al IV. For Fe XVII, the $2s2p^63p$, $4p$, $5p$, and $6p$ levels are bound, so that $2s2p^67p$ is the first autoionizing state.

In addition to scaling considerations for the autoionizing contribution, there must also be consideration of stabilization of the autoionizing configuration via radiative decay, such as $2s2p^63p\rightarrow 2s^22p^53p$ or $2s2p^63p-2s^22p^6$. Such radiative stabilization would decrease the influence of the excitation-autoionization process on the total ionization cross section.

Owing to the lack of quantitative information on the branching ratios for radiative stabilization and autoionization, we have not included the excitation-autoionization process in the total cross sections listed in Table III. Calculations for Al IV, where the effect should be large compared to other ions in the sequence, indicate less than a 2% increase in total cross sections assuming 100% autonization. This estimate includes a sum over excitation to higher $2s2p^6np$ levels using

an $(n^*)^{-3}$ extrapolation rule based on distorted-wave exchange calculations of the $2s^22p^6 - 2s2p^6\,3p$ excitation.

C. Comparison to experimental and other theoretical results

Experimental cross section data for neon-like ions are currently available only for Na^+(Refs. 9 and 10) and Mg^{++}.[11] Figure 8 shows the ratio of the present distorted-wave Born-exchange results to a fit made to the experimental points. Although there is a significant discrepancy between theory and experiment at low impact energies, for $u > 1.8I_{2p}$ both ratios appear to be approaching asymptotic values of ~1.4 for Na^+ and ~1.3 for Mg III. Convergence with increasing Z might be anticipated assuming the theory is correct in the high-Z limit.

Moores[21] has performed Coulomb-Born no-exchange calculations for Na^+ and Mg^{++} using distorted-wave ejected partial waves. His data are in good agreement with present distorted-wave no-exchange results, but are about 10% higher than the distorted-wave Born-exchange points.

The scaled hydrogenic ($Z=\infty$) approximation[25] for electron-impact ionization has been applied to a number of orbitals, including the $2p$ and $2s$ of interest here. Figure 9 is a comparison of the results obtained via this simple method to the present distorted-wave Born-exchange results. As expected, agreement is poor for low charge states but improves rapidly with increasing Z. For $Z > 17$, $Q(Z=\infty)/Q(\mathrm{DB}) < 1.25$. Note that the $Z=\infty$ cross sections shown were computed by the author in the maximum exchange scattering

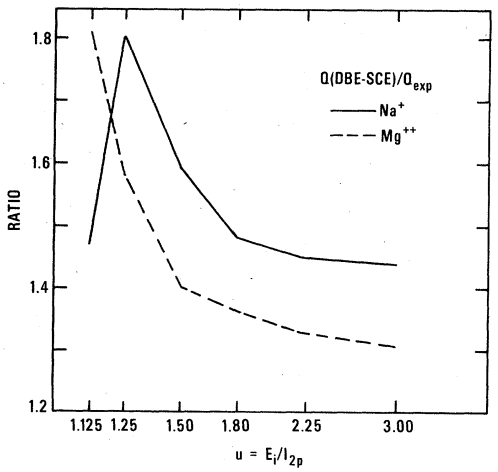

FIG. 8. Ratio of the present distorted-wave Born-exchange total ionization cross sections to the experimental results of Refs. 9, 10, and 11.

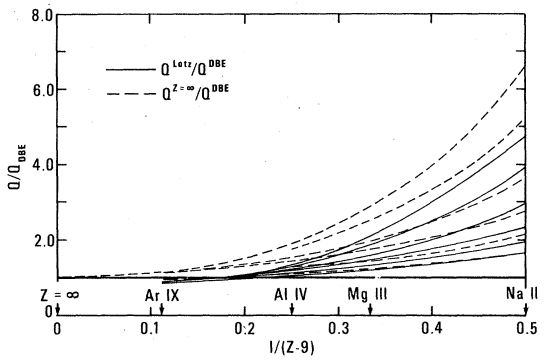

FIG. 9. Ratio of the semiempirical ionization cross sections of Lotz (Ref. 20) (solid curves) and scaled hydrogenic cross sections to the present distorted-wave Born-exchange results for the neon isoelectronic sequence. For $Z=\infty$ the present results will agree exactly with the scaled hydrogenic approximation.

approximations and thus differ by a few percent from the data of Ref. 25, which were computed using the phase convention of Rudge and Schwartz[3] for the exchange matrix element. As a check, cross sections were generated in the later approximation; in all cases agreement with the results of Ref. 25 was obtained to within the number of significant figures quoted.

Also in Fig. 9 is a comparison of the Lotz semiempirical formula[20] used often in plasma modeling studies to the DBE data. The disagreement at low charge states is somewhat misleading since the "universal" cross-section formula given by Lotz:

$$uI^2Q = (2.77 \ln u)(\pi a_0^2\ \mathrm{Ry}^2) \qquad (7)$$

per subshell electron should be restricted to effective ionic charges greater than three. For the first three ions Lotz gives more detailed parametrizations derived from experimental cross-section data. It is not surprising that the Lotz semiempirical parametrizations so accurately reproduce experimental data for low ionization stages, since they are merely fits to the available data. [Equation (7) differs from other simple formulas for the electron-impact-ionization cross section in that it is deduced from actual measurements, and not classical extrapolations. As such it constitutes a useful comparison for *ab initio* calculations. Its obvious drawback, however, is that it is limited to gross predictions of the cross section, and is incapable of yielding detailed information on complex ions for which no experimental data are yet available. Also, the Z-scaling law upon which Eq. (7) is based, i.e., classical scaling by the square of the ionization energy, has been verified only

for a very limited number of simple isoelectronic sequences.

D. Other effects

The significant discrepancy between the DBE and experimental cross sections for Na^+ led to the investigation of a number of possible improvements in the basic DBE approximation for the calculation of total ionization cross sections. Some of these are described below.

(1) Term dependence in the potential used to generate the ejected partial wave. The well-known ^1P exchange interaction in the $2p^5Kl$ configuration was approximated within the semiclassical exchange approximation. At $u=1.25$, the ratio $Q^{\text{theory}}/Q^{\text{expt}}$ for Na^+ decreased to 1.45 from 1.8; but at $u=3$, the effect was only a few percent.

(2) Angular coupling in the final state. Assuming term independence of the radial orbitals and ionization energies, the sum rules of Racah result in DBE cross sections independent of the coupling scheme chosen for individual final-state terms.[1]

(3) Knockout: Exchange between the incident electron and the target should be dominated by the incident p-wave cross section, which in itself is insufficient to account for the observed discrepancy.

(4) Final-state continuum-continuum interaction. Interaction between the two final-state electrons, both of relatively low energy, could pose a serious problem for the calculation of electron-impact-ionization cross sections by simple methods based on first-order perturbation theory, such as the present DBE method. Evidence that such interactions may not be critical for incident energies away from threshold is found in earlier calculations made for the lighter isoelectronic sequences H, He, and Li. Better agreement between theory and experiment was obtained in all of these simple isoelectronic sequences than in the Ne sequence, despite the presence of the same qualitative continuum-continuum final-state interaction.

(5) Scattering representation. The insensitivity of the total cross section to the incident and final scattered waves, and the sensitivity to the ejected waves, points to a fundamental separation of the scattering matrix into target and scattering parts. If such a separation was applied, it would allow techniques developed for photoionization calculations to be carried over to the more complex electron-impact problem.

V. CONCLUSION

Electron-impact-ionization cross sections for four ions in the neon isoelectronic sequence have been computed in the distorted-wave Born-exchange approximation. Significant departures from classical scaling by the square of the ionization energy were noted for low ionization stages. Total cross sections were found to be sensitive to the description of the ejected partial waves, but were quite insensitive to details of the scattered waves. Comparison of the present results for Na^+ and Mg^{++} to experimental data indicated discrepancies much larger ($>30\%$) than were observed in parallel calculations for light isoelectronic sequences, and indicate a need both for improved representation of the ejected partial waves as well as a more rigorous formulation of the theory of electron-impact ionization itself. Investigations concerning both of these areas are currently under way.

ACKNOWLEDGMENT

This work was supported in part by the Department of Energy, Office of Magnetic Fusion Energy.

[1] M. R. H. Rudge, Rev. Mod. Phys. 40, 564 (1968).
[2] A. Burgess, H. P. Summers, D. M. Cochrane, and R. W. P. McWhirter, Mon. Not. R. Astron. Soc. 179, 275 (1977).
[3] M. R. H. Rudge and S. B. Schwartz, Proc. Phys. Soc. London 88, 563 (1966).
[4] S. M. Younger, Phys. Rev. A 22, 111 (1980).
[5] S. M. Younger, Phys. Rev. A 22, 1425 (1980).
[6] H. Jakubowicz and D. L. Moores, Comments At. Mol. Phys. (in press).
[7] E. Stingl, J. Phys. B 5, 1160 (1972).
[8] B. L. Schram, A. J. H. Boerboom, and J. Kistemaker, Physica (Utrecht) 32, 185 (1966).
[9] J. W. Hooper, W. C. Lineberger, and F. M. Bacon, Phys. Rev. 141, 165 (1966).
[10] B. Peart and K. T. Dolder, J. Phys. B 1, 240 (1968).
[11] B. Peart, S. O. Martin, and K. T. Dolder, J. Phys. B 2, 1176 (1969).
[12] M. E. Riley and D. G. Truhlar, J. Chem. Phys. 63, 2182 (1975).
[13] E. Clementi and C. Roetti, At. Data Nucl. Data Tables 14, 177 (1974).
[14] R. K. Peterkop, Zh. Eksp. Teor. Fiz. 41, 1938 (1961) [Sov. Phys.–JETP 14, 1377 (1962)].
[15] C. E. Moore, *Ionization Potentials and Ionization Limits Derived from Analyses of Optical Spectra*, Natl. Stand. Ref. Data Ser., Natl. Bur. Stand. (U.S.) Circ. 34 (1970).
[16] T. B. Lucatorto and T. J. McIlrath, Phys. Rev. Lett. 7, 428 (1976).

[17]W. C. Martin and R. Zalubas, J. Phys. Chem. Ref. Data 9, 1 (1980).
[18]W. C. Martin and R. Zalubas, J. Phys. Chem. Ref. Data 8, 817 (1979).
[19]A. W. Weiss (private communication).
[20]W. Lotz, Z. Phys. 216, 241 (1968).
[21]D. C. Moores, J. Phys. B 5, 286 (1972).
[22]A. L. Merts, J. B. Mann, W. D. Robb, W. H. Magee, Jr., and M. F. Argo, Atomic Data Workshop–Preliminary Report, Los Alamos Scientific Laboratory, Los Alamos, New Mexico, 1978 (unpublished).
[23]A. Chutjian and L. D. Thomas, Phys. Rev. A 11, 1583 (1975).
[24]J. J. Thomson, Philos. Mag. 23, 449 (1912).
[25]D. L. Moores, L. B. Golden, and D. H. Sampson, J. Phys. B 13, 385 (1980).